ABS ACTA BIOLOGICA SIBIRICA
A journal on the biodiversity of Siberia and the adjacent lands

Acta Biologica Sibirica 11: 833–845 (2025)
doi: 10.5281/zenodo.16743967
http://journal.asu.ru

RESEARCH ARTICLE

Differential expression of the multiplicated silicon transporter genes at different stages of morphogenesis of daughter frustule of the freshwater diatom *Ulnaria acus*

Artem M. Marchenkov[1], Yulia R. Zakharova[1], Darya P. Petrova[1]

1 *Limnological Institute, Siberian Branch of the Russian Academy of Sciences, 3 Ulan-Batorskaya st., Irkutsk, 664033, Russia*

Corresponding author: Artem M. Marchenkov (marchenkov.am@gmail.com)

Academic editor: R. Yakovlev | Received 20 June 2025 | Accepted 7 July 2025 | Published 7 August 2025

http://zoobank.org/7012DCAC-496C-44D7-8BBE-347D129FF334

Citation: Marchenkov AM, Zakharova YuR, Petrova DP (2025) Differential expression of the multiplicated silicon transporter genes at different stages of morphogenesis of daughter frustule of the freshwater diatom *Ulnaria acus*. Acta Biologica Sibirica 11: 833–845. https://doi.org/10.5281/zenodo.16743967

Abstract

Diatoms are known for their unique ability to form species-specific silicon exoskeletons (shells) richly decorated with various ornaments, outgrowths, and holes. The absorption of silicic acid from the environment by cells is a critical step in this process. It is known that silicic acid is transported into diatom cells by silicic acid transport proteins (SIT). However, the mechanism and regulation of the work of proteins of this family currently remain insufficiently studied. In the present study, we attempted to determine the stages of daughter valve morphogenesis in the pennate freshwater diatom *Ulnaria acus* and to assess the expression level of *sit-m* genes encoding multiplexed silicon transporters. The experiment showed that simultaneously with the formation of the main axial element of the daughter valves (sternum) and first-order branching (virga), the level of *sit-tri* gene expression increases. While, during the formation of second-order branching (vimin) and areoles, an increase in the level of *sit-td* gene expression was noted, with a simultaneous decrease in *sit-tri*. Based on the data obtained, it can be assumed that after duplication of *sit* genes in the diatom genome, with the formation of multiplexed structures, their subfunctionalization occurs at different stages of daughter valve morphogenesis.

Keywords

Diatom, silicic acid transporters (SITs), valve morphogenesis, gene expression

Introduction

Silicon is the second most abundant chemical element in the Earth's crust after oxygen. In the aquatic environment, dissolved silicon is present in various chemical forms, usually designated as $SiO^x(OH)^x2$. The most common form is silicic acid $Si(OH)4$. Between 200 and 280^x10^{12}mol Si/yr of biogenic silica are produced in the ocean annually (Nielsen 2014). A key role in this process is played by diatoms (Bacillariophyta). These single-celled eukaryotes are one of the ecologically important groups, including because they dominate among photosynthetic organisms (Malviya et al. 2016). Modern diatom taxonomy is based on the fine structure and symmetry of their shells and includes between 18 211 (Guiry 2024) and an estimated 100 000 species (Mann and Vanormelingen 2013).

There is currently no complete understanding of how genetically programmed mechanisms are able to create physical and chemical interactions that control the morphogenesis of complex mineral structures. The process of uptake and transport of silicic acid into diatom cells is one of the important stages of the morphogenesis of daughter valves. The silicon content in the waters of the world's oceans averages 70 μM (Tréguer et al. 1995), while inside the cell it reaches 150 mM (Kumar et al. 2020). At the same time, during the morphogenesis of the valve, the cell must absorb a sufficient amount of silicon in a short time. When the level of silicic acid in the environment is insufficient, depending on the diatom species, the cell cycle stops in the G1, G2 or M phase and the cells begin to store nutrients, which can then be used for division and growth (Brzezinski et al. 1990; Cavonius et al. 2015; Hildebrand et al. 2007; Martin-Jezequel et al. 2000). Thus, the capture of silicon from the environment and its transport into the diatom cell is a strategically important process for these organisms.

It was shown that with increasing concentration of silicic acid in the nutrient medium, the rate of silicon (or its close analogue germanium, Ge) incorporation into diatoms and the growth rate of the culture (the number of cell divisions per unit time) initially increased, and with further increase in concentration they reached a plateau (Sullivan 1977). This suggested that an agent obeying the Michaelis-Menten law is involved in silicon utilization (Azam et al. 1974). An important achievement in understanding this process is the identification of the silicon transporter (SIT) protein in the marine diatom *Cylindrotheca fusiformis* (Hildebrand et al. 1997). It was possible to establish the nucleotide sequence of five genes that form a closely related family. Predicted amino acid sequences from nucleotide sequences showed that the corresponding proteins are good candidates for the role of silicic acid transporters (Hildebrand et al. 1998).

Currently, *sit* genes represent a family of paralogs and are found in various organisms of different taxa (Thamatrakoln and Hildebrand 2007; Grachev et al. 2002; Likhoshway et al. 2006; Marron et al. 2013; Durkin et al. 2016; Marron et al. 2016; Sapriel et al.; 2009 Marchenkov et al. 2018; Bryłka et al. 2023; Kim et al. 2024). In most species, 3-5 copies of genes of this family were found in the genome (Hildebrand et al. 1997; Alverson 2007; Thamatrakoln et al. 2006; Durkin et al. 2016).

Based on the structure, three groups can be distinguished in the *sit* gene family: *sit-l* encode proteins consisting of 5 TM, *sit-encode* proteins of 10 TM, and *sit-m* encode multiplicated proteins of 20–30 TM (Durkin et al. 2012; Marron et al. 2016; Marchenkov et al. 2018). Based on the results of structural and phylogenetic analyses, it has been suggested that the *sit* genes were formed as a result of intragenic duplication (Thamatrakoln and Hildebrand 2007; Bryłka et al. 2023). Using phylogenetic analysis, SIT proteins were divided into five clades (A-D), which, as the authors suggest, reflect their affinities for silicic acid (Durkin et al. 2016).

Recently, *sit* gene expression has been studied in marine and some freshwater centric diatoms. Much attention has been paid to understanding at which stages of the cell cycle individual paralogs are expressed (Hildebrand et al. 1998; Thamatrakoln and Hildebrand 2007; Bryłka al. 2023) or what conditions can affect the expression of these genes. Lack of nitrogen and silicon in the culture medium are considered as factors (Durkin et al. 2016; Kim et al. 2024). However, all these studies are focused on understanding the function of *sit* genes encoding proteins with 10 TM domains. Since we have previously identified genes encoding SIT-M proteins in freshwater pennate diatoms and described the structure of the cluster encoding their genes in the genomes of two species of the genus *Ulnaria*, it is of interest at what stages of morphogenesis of daughter valves the activation of *sit-m* genes occurs.

In our work, we analyzed for the first time the expression of *sit-m* genes in the freshwater pennate diatom *Ulnaria acus* (Kützing) Aboal. Although the study only touches upon the work of multiplexed SIT-M proteins, it provides important information about the strictly coordinated work of paralogs of this family not only at the stages of the cell cycle, but also at different stages of morphogenesis of daughter valves. The obtained results allow us to come closer to understanding the general patterns of morphogenesis in diatoms.

Materials and methods

Cultivation conditions

An axenic monoclonal strain of the pennate araphid freshwater diatom *Ulnaria acus* (Kützing) M. Aboal BK497 was isolated in February 2020 from an under-ice phytoplankton sample near the settlement of Bol'shiye Koty (Lake Baikal, Russia) according to the method described earlier (Shishlyannikov et al. 2011). Cells were grown in sterile Diatom Medium (DM) (Thompson 1988) in 100 ml Erlenmeyer flasks at 8 °C and 16 μmol/m2/s illumination with a day/night cycle (12:12). Axenicity of the culture was checked by DAPI staining using an Axiovert 200 microscope (Zeiss, München, Germany) and a UV filter.

Cell synchronization

The biomass of the cells was then filtered through analytical track-etched membranes filters with 3μm pores (Reatrack, Russia) The cells were transferred to a silicon-free medium, where they were cultured for 72 hours in the dark. Cells were synchronized according to the protocol published earlier (Bedoshvili et al. 2019). After three days of culturing, *U. acus* were concentrated using a filter and the cells were placed in DM medium with silicon. The cell biomass for RNA extraction was collected after 30, 60, 90, 120 and 180 min, also before adding silicon. In order to increase the preservation of RNA, the biomass was fixed with IntactRNA solution (Eurogen, Russia), according to the manufacturer, after which the components were stored at – 80 ˚C.

RNA Isolation and cDNA Synthesis

To isolate RNA, the samples were defrosted and centrifuged at 5,000 g for 5 min, then the supernatant was removed. The cells were transferred to nitrogen-cooled mortars and ground to a homogeneous state. After evaporation of liquid nitrogen, RLT buffer was added and RNA was isolated using the RNeasy Plant Mini Kit (Qiagen, Germany), according to the manufacturer's instructions. The isolated RNA preparations were treated with 3U DNase I (Thermo Fisher Scientific, USA) for 60 min at 37 ˚C. DNase inactivation was performed using 6 μl DNase Inactivation Reagent (Thermo Fisher Scientific, USA) for 5 min at room temperature, then centrifuged for 1.5 min at 10 000 g, the supernatant was collected and used for the synthesis of the first strand of cDNA. cDNA synthesis was performed in 20 μl of a reaction mixture containing 1x First strand buffer, about 200 ng of total RNA treated with DNase I, a mixture of dNTPs (1 mM each), 1 μM oligo-(dT)18 primer, 1 mM DTT, 20 units of RiboLock RNase inhibitor (Thermo Scientific, USA), and 100 units of MMLV reverse transcriptase (Eurogen, Russia). The reaction was carried out for 60 min at 37 °C. Reverse transcriptase was inactivated for 10 min at 70 °C. To control DNA contamination, a reaction without the addition of transcriptase (NoRT) was performed.

Real-Time PCR and Statistical Analysis

For real-time PCR, primers for *sit-tri* and *sit-td* genes (Table 1) were used, which were selected based on the previously published sequence of KX345281.2 (Marchenkov et al. 2016). 18S rRNA was used as a reference gene (Liu et al. 2020), and primers were used from a previously published work (Table 1, Bayramova et al. 2024).

The amplification reaction was carried out in 20 μl and the mixture contained (1x reaction buffer, 1.25 units of Taq DNA polymerase activity, 0.2 mM dNTP mix, 2.5 mM Mg^{2+}, 0.2 μM each of primers, 0.2 μl SYBR Green I, 0.4 μl ROX, 1 μl (reac-

tion mix after reverse transcription). The reaction temperature profile was as follows: 95 °C for 3 min, 40 cycles (95 °C for 30 sec, 57 °C for 20 sec, 72 °C for 20 sec). A reaction mix without cDNA was used as a negative control. Each real-time PCR was done in triplicate to calculate the standard deviation.

The relative gene expression was assessed via reference gene valuation followed with the delta-delta Ct method (Livak and Schmittgen 2001). Data was presented as mean ± standard deviation and was analyzed using two-way ANOVA (Fig. 3; Table 2) and two-sample t-test (Table 2).

Table 1. Primer sequences for real-time PCR

Gene	Primer	Sequence 5′→3′
sit-tri	Uasit-tri_QPCR_7408F	GTAGACGAGAAAGAGAATGTTGAGG
	Uasit-tri_QPCR_7506R	AGAGAGGATGAGCAATACGGTG
sit-tri/sit-td	Uasit_QPCR_11189F	AGACATTTTTGAATACGGGACTGA
	Uasit_QPCR_11334R	AAGCAGCAAACAAACTCTGATGA
18S rRNA (LSU)	18S_QPCR_1316F	CTTCTTAGAGGGACGTGCGTTC
	18S_QPCR_1445R	TCTCGGCCAAGGTACACTCG

Table 2. Marginal means of *sit* and *sit-tri* values of different groups and their effect over time (two-way ANOVA and two-sample t-test)

	SS between groups	SS within the group	F	P-value	t-statistics	Dispersion
0 min	0.815	0.032	49.55	0.019	4.01	0.166
30 min	6.367	0.301	42.28	0.02	-6.04	0.196
60 min	3.19	0.26	24.15	0.03	-6.56	0.001
90 min	124.24	1.23	201.53	0.004	19	1.1
120 min	39.16	0.09	797.45	0.001	4.15	11.82
180 min	3.96	1.53	5.15	0.15	1.33	1.2

Scanning electron microscopy (SEM)

Scanning electron microscopy (EM) was used to analyze the stages of morphogenesis and determine the proportion of daughter cells. From each sample, 50 µl of sediment were taken and treated with 6 % SDS for 30 min at 95 °C, then washed five times with distilled water. The sediment was incubated with concentrated nitric acid for 60 min at 95 °C, washed three times with ethanol and kept for 24 hours with 36 % hydrochloric acid. After treatment, the sediment was washed five times with distilled water and resuspended in 500 µl of 70 % ethanol, applied to SEM tables, dried at room temperature and sputtered with gold. The suspension of cleaned valves was pipetted onto a coverslip, dried, mounted on a stub for SEM, and examined in a QUANTA 200 scanning electron microscope (FEI, United States). in the Collective

instrumental center "Ultramicroanalysis" at the LIN SB RAS. The counting of dividing valves was performed in three replicates among 100 randomly encountered valves. The counting of valves at different stages of morphogenesis was carried out according to the features described previously (Kaluzhnaya and Likhoshway 2007; Kharitonenko et al. 2015).

Results

Identification of daughter valves and understanding of the dynamics of their formation in *U. acus* were carried out in the first 3 hours after adding cells to a silicon-containing medium. It should be noted that after 72 hours of cultivation in a silicon-free medium, approximately 18 % of the cells formed new valves (Fig. 1). However, most of the forming valves were at the last stages IV and V (Fig. 2), when vimins (second-order branches) and areoles are formed, and valves thicken. This may be due to a slowdown in the formation of daughter valves in the absence of silicon in the medium.

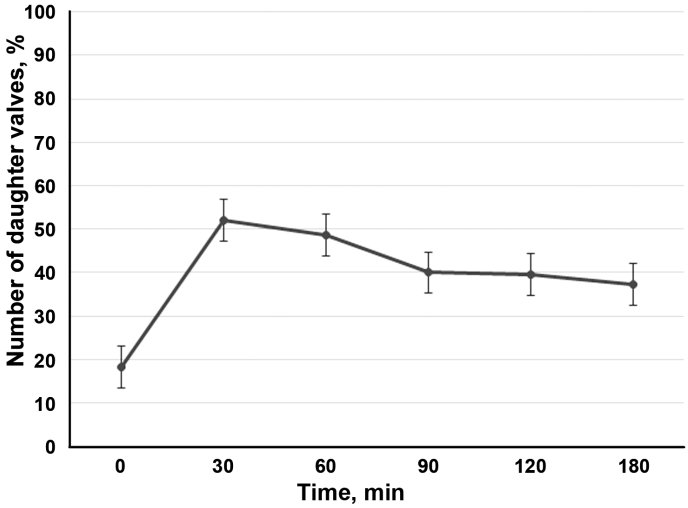

Figure 1. Total number of daughter valves relative to the total number of valves after synchronization (0) and after cultivation in a medium with silicon (30, 60, 90, 120 and 180 min).

Thirty minutes after adding the silicon-containing medium to the cells, an increase in the number of daughter valves to 54.5 % was observed (the maximum number of daughter valves for the entire experiment) (Fig. 1). Most of the daughter valves were at stage II of morphogenesis. 10 % of the daughter valves were at stage I

with the formation of the sternum (Fig. 2A, B). At the same time, a decrease in the number of valves at later stages was noted (Fig. 2F, G). Similar dynamics were described earlier for *U. danica* (Bedoshvili et al. 2019). Over the next 60 min, a gradual decrease in the number of valves was observed at the first stages of morphogenesis and an increase in the number of valves at stage IV, and then at stage V, during which the formation of second-order branching (vimin) and the formation of areoles occurs (Fig. 3A, E, G). After 120 minutes from the beginning of the experiment, the number of valves of stages II and III increased again, while the number of cells at stage IV decreased (Fig. 3A, C–E). After 180 min from the addition of cells to the silicon-containing medium, desynchronization of division occurred (Fig. 3A). Thus, the formation of the main valve structures in *U. acus* occurs within the first two hours, as in another representative of the genus *Ulnaria* – *U. danica* (Bedoshvili et al. 2019).

Analysis of the expression level showed that before adding silicic acid to the medium, the transcription level of the *sit-tri* and *sit-td* genes in synchronized cells is approximately at the same level (Fig. 3). 30 min after adding silicic acid to the DM, active division begins and the formation of daughter valves is accompanied by an insignificant increase in the expression level of the *sit-tri* gene and a decrease in *sit-td* (Fig. 3). After 60 min, the virgi expand and a valve bend is formed in most daughter valves, while the transcript levels of both genes remain at the same level. A sharp increase in the *sit-td* gene expression level (13-fold) is recorded at 90 min during the formation of vimin and areoles, while the *sit-tri* level decreases 14-fold (Fig. 3). After 120 min, the *sit-td* gene expression level decreases by 30 % (Fig. 3). After another 60 min, when the daughter valves are fully formed and gradually thicken, and the sternum is laid down in the new valves, the level of *sit-td* gene transcripts decreases by 2 times, and the level of *sit-tri* expression increases by more than 13 times (Fig. 3).

After statistical evaluation of the expression level of *sit-td* and *sit-tri* genes, it is seen that the level of dispersion begins to increase after 90 min and reaches a maximum at 120 min, and then it decreases (Table 2). The maximum level of the t-statistics value is observed at 90 min, and at 120 min the level of the t-statistics has almost the same value as at 0 min (Table 2).

Discussion

In recent years, diatoms have attracted increasing attention because understanding the cellular mechanisms underlying biomineralization may be promising for use in various applications. As is known, one of the decisive roles in this process is played by SIT proteins, facilitating the import and intracellular transport of dissolved silicon. It is important to understand the mechanisms that control Si absorption during active formation of daughter valves, when free diffusion of silicon is insufficient.

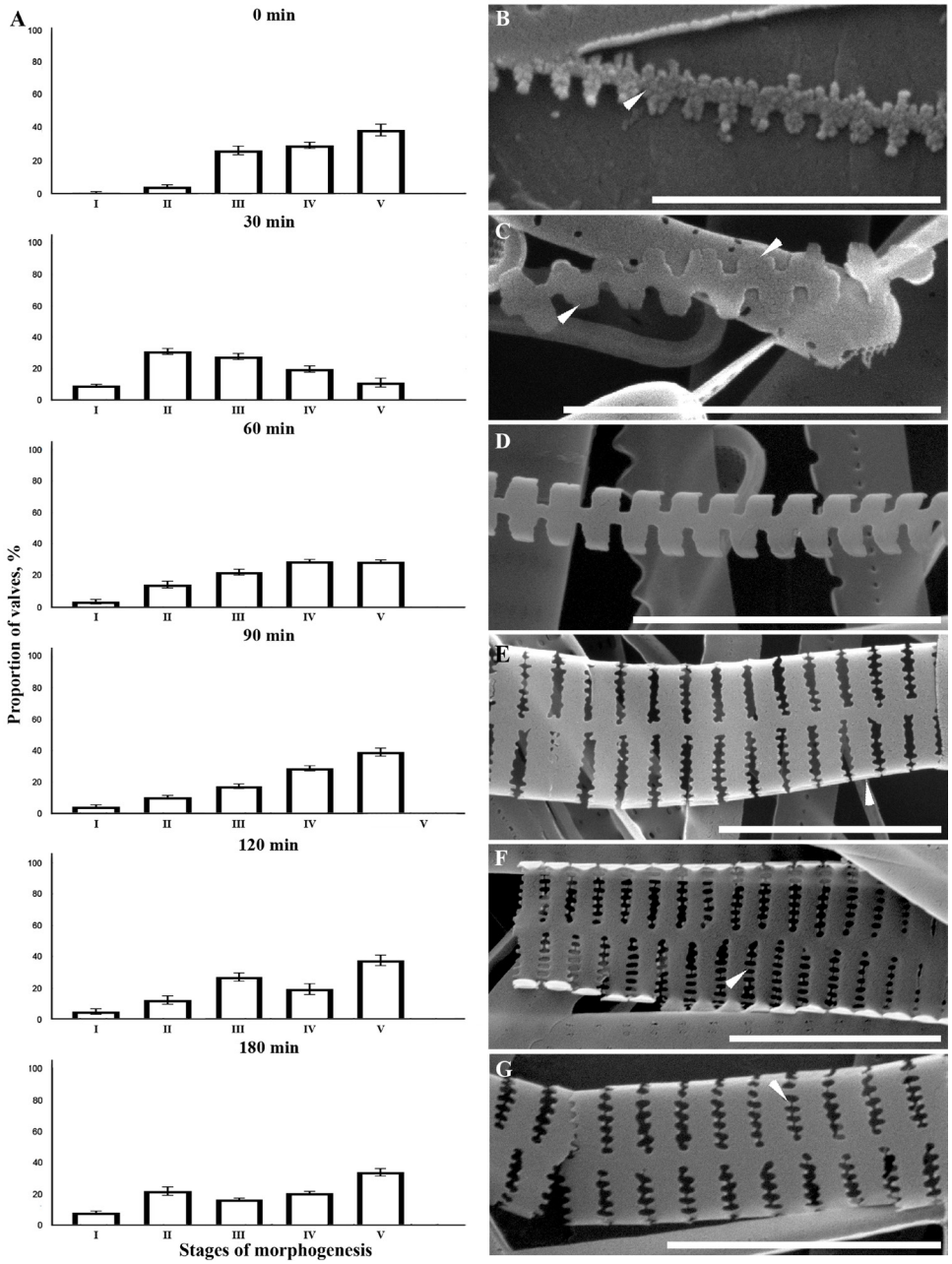

Figure 2. Daughter valves of *U. acus* at different stages of morphogenesis. **A** – Proportions of daughter valves at different stages of morphogenesis (here and below, relative to the total number of valves examined) at different time points; **B** – stage I, formation of sternum; **C** – stage II, formation of virgae (branches from sternum of the first order); **D** – stage III, growth of virgae to the valve mantle; **E** – stage IV, formation of viminae (second-order branches); **F** and **G** – stage V, formation of areolae from the inside and outside of the valve, respectively. SEM. Scale bars: **B** and **C** 2 μm; **D** and **G** 5 μm. Error bars indicate standard deviations.

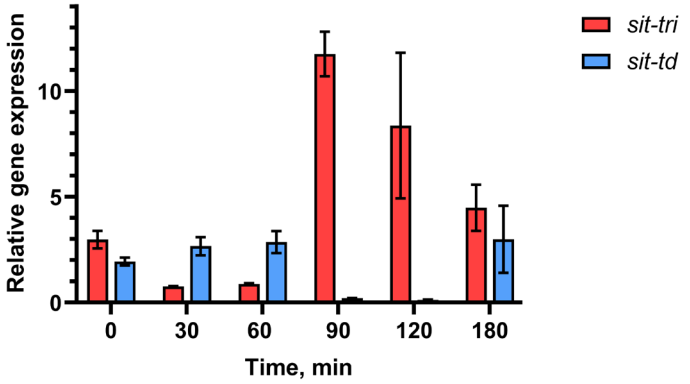

Figure 3. Change in relative levels of *sit-tri* (red column) and *sit-td* (blue column) gene expression in a synchronized *U. acus* culture before (0 min) and after addition of silicon-containing medium (30 min, 60 min, 90 min, 120 min, 180 min). Data on *sit-tri* and *sit-td* gene expression are presented in multiples. Means with different letters were significantly different ($p < 0.05$). Error bars indicate mean with SD (two-way ANOVA).

The cell cycle of *U. acus* is about 24 hours. It is known that the general structural plan of daughter valves in the morphologically similar species *F. radians* (formerly known as *Synedra acus* subsp. *radians*) is formed during the first 3.5 hours after the addition of silicon, whereas the main part of the primary morphogenesis of the closely related species *U. danica* occurs within 2 hours (Kaluzhnaya and Likhoshway 2007; Kharitonenko et al. 2015). In connection with these data, it is relevant to study the expression of silicon transporters in the first 3 hours after the addition of silicon to the medium.

Our study provided the first information on the behavior of silicon transporters during sternum initiation and subsequent valve formation. Comparison of molecular biology data and SEM analysis of daughter valve formation dynamics allowed us to establish that SIT-TRI and SIT-TD proteins are active at different stages of daughter valve morphogenesis. SIT-TRI is involved in the initial stages of morphogenesis during initiation of a new valve and formation of first-order branching, whereas SIT-TD is more active at later stages during formation of vimins (second-order branching), areolas, and gradual thickening of the daughter valve. This is consistent with and expands on previously proposed assumptions about the method of silicon uptake control – induction and suppression of transport activity during certain periods of the cell cycle (Sullivan, 1977). Thus, control of the activity of silicon uptake and transport depends not only on the stages of the cell cycle, but also on the stages of morphogenesis, the passage of which can be greatly delayed with a deficiency of intracellular silicon. This is confirmed by the fact that in the *U. acus* culture, after 72 hours of incubation in a silicon-free medium, valves were found at late stages of morphogenesis IV and V.

As is known, the predicted amino acid sequence of SIT-TD of *U. acus* consists of two domains SIT1B and SIT2, and the predicted amino acid sequence of SIT-TRI of *U. acus* consists of three domains SIT1A, SIT1B and SIT2. When pairwise comparing the domains SIT1B of SIT-TD and SIT1B of SIT-TRI and SIT2 of SIT-TD and SIT2 of SIT-TRI, they are identical, thus, SIT-TRI differs from SIT-TD by the presence of the domain SIT1A at the C-terminus (Marchenkov et al., 2016). It remains unclear whether individual SIT domains can undergo subfunctionalization and have, for example, different affinity for silicic acid or different intracellular localization.

Recently, data have been obtained for genes encoding non-multiplicated SIT proteins in several marine diatoms (Hildebrand et al. 1997; Sapriel et al. 2009; Thamatrakoln and Hildebrand 2007; Shrestha et al. 2012). Such proteins are similar in structure to individual SIT-M domains. Different paralogs of these *sit* genes have different transcription levels at different periods of the cell cycle. For example, three *sit* genes were found in *Thalassiosira pseudonana* Hasle & Heimdal; when assessing their expression levels, it was shown that the expression level of all three genes was highest 180 min after the addition of silicic acid to the medium in the S-phase during the formation of girdle rims, but before the formation of the daughter valve. The expression level of the *sit3* gene is significantly lower than the expression levels of *sit1* and *sit2*. The authors suggest that the SIT3 protein acts as a sensor for silicic acid rather than a transporter (Thamatrakoln and Hildebrand 2007). Similar results were obtained in the analysis of transcriptome data in this species (Shrestha et al. 2012). Five paralogs of this family were found in the genome of the marine diatom *Cylindrotheca fusiformis* Reimann & J.C. Lewin, and the expression of all *sit* was induced simultaneously, immediately before the period of maximum silicon deposition in the cell wall, and the levels decreased by the end of this period (Hildebrand et al. 1998). When assessing the expression level of *sit* genes in *Thalassiosira eccentrica* (Ehrenberg) Cleve 1904, it was shown that the expression level of the *sit3* gene remained almost unchanged during the cell cycle, while the expression level of *sit1/2* genes initially increased sharply, then reached a plateau and decreased by the end of the experiment. The authors of the work suggest that the *sit* genes of *T. eccentrica* have different intracellular localizations, one of the *sit* genes is located on the cytoplasmic membrane and transfers silicic acid into the cell, while the other is involved in intracellular regulation (Kim et al. 2024). The assumption about different localizations of SIT proteins in diatom cells can be indirectly confirmed by previously obtained data on the expression of the chimeric protein SIT2-GFP *Phaeodactylum tricornutum* Bohlin 1898 in cells, where it was shown that the protein is localized in the cytoplasmic membrane (Sapriel et al. 2009).

Thus, in our work, the activity of *sit-m* genes was shown for the first time using the pennate freshwater diatom *U. acus* as an example. Understanding how silicic acid is absorbed at different stages of daughter valve morphogenesis using different representatives of the silicon transporter family will allow us to approach the deciphering of the general patterns of species-specific morphogenesis.

Acknowledgements

The research was funded by the Ministry of Science and Higher Education of the Russian Federation, project number 121032300191-3.

References

Alverson AJ (2007) Strong purifying selection in the silicon transporters of marine and freshwater diatoms. Limnology and Oceanography 52(4): 1420–1429. https://doi.org/10.4319/lo.2007.52.4.1420

Azam F, Hemmingsen BB, Volcani BE (1974) Role of silicon in diatom metabolism: V. Silicic acid transport and metabolism in the heterotrophic diatom *Nitzschia alba*. Archives of Microbiology 97: 103–114. https://doi.org/10.1007/BF00403050

Bayramova E, Petrova D, Marchenkov A, Morozov A, Galachyants, Y, Zakharova Y, Bedoshvili Y, Likhoshway Y (2024) Differential Expression of Stress Adaptation Genes in a Diatom *Ulnaria acus* under Different Culture Conditions. International Journal of Molecular Sciences 25: 2314. https://doi.org/10.3390/ijms25042314

Bedoshvili YeD, Volokitina NA, Marchenkov AM (2019) Valve morphogenesis and silicon dynamics in the synchronized culture of *Ulnaria danica*. Limnology and Freshwater Biology 5: 297–301. https://doi.org/10.31951/2658-3518-2019-A-5-297

Bryłka K, Pinseel E, Roberts WR, Ruck EC, Conley DJ, Alverson AJ (2023) Gene duplication, shifting selection, and dosage balance of silicon transporter proteins in marine and freshwater diatoms. Genome Biology and Evolution 15(12): evad212. https://doi.org/10.1093/gbe/evad212

Brzezinski MA, Olson RJ, Chisholm SW (1990) Silicon availability and cell-cycle progression in marine diatoms. Marine Ecology Progress Series 67: 83–96.

Cavonius L, Fink H, Kiskis J, Albers E, Undeland I, Enejder A (2015) Imaging of lipids in microalgae with coherent anti-stokes Raman scattering microscopy. Plant physiology 167(3): 603–616. https://doi.org/10.1104/pp.114.252197

Durkin CA, Marchetti A, Bender SJ, Truong T, Morales R, Mock T, Armbrust E (2012) Frustule-related gene transcription and the influence of diatom community composition on silica precipitation in an iron-limited environment. Limnology and Oceanography 57(6): 1619–1633. https://doi.org/10.4319/lo.2012.57.6.1619

Durkin CA, Koester JA, Bender SJ, Armbrust E (2016) The evolution of silicon transporters in diatoms. Journal of Phycology 52(5): 716–731. https://doi.org/10.1111/jpy.12441

Grachev MA, Denikina NN, Belikov SI, Likhoshvai EV, Usoltseva MV, Tikhonova IV, Shcherbakova TA (2002) Elements of the active center of silicon transporters in diatoms. Molecular Biology 36: 534–536. https://doi.org/10.1023/A:1019860628910

Guiry MD (2024) How many species of algae are there? A reprise. Four kingdoms, 14 phyla, 63 classes and still growing. Journal of Phycology 60(2): 214–228. https://doi.org/10.1111/jpy.13431

Hildebrand M, Volcani BE, Gassmann W, Schroeder JI (1997) A gene family of silicon transporters. Nature 385: 688–689. https://doi.org/10.1038/385688b0

Hildebrand M, Dahlin K, Volcani BE (1998) Characterization of a silicon transporter gene family in *Cylindrotheca fusiformis*: sequences, expression analysis, and identification of homologs in other diatoms. Molecular Genetics and Genomics 260: 480–486. https://doi.org/10.1007/s004380050920

Hildebrand M, Frigeri LG, Davis AK (2007) Synchronized growth of *Thalassiosira pseudonana* (Bacillariophyceae) provides novel insights into cell-wall synthesis processes in relation to the cell cycle. Journal of Phycology 43: 730–740. http://dx.doi.org/10.1111/j.1529-8817.2007.00361.x

Kaluzhnaya OV, Likhoshway YV (2007) Valve morphogenesis in an araphid diatom *Synedra acus* subsp. *radians*. Diatom Research 22(1): 81–87. https://doi.org/10.1080/0269249X.2007.9705696

Kharitonenko KV, Bedoshvili YeD, Likhoshway YeV (2015) Changes in the micro- and nanostructure of siliceous frustule valves in the diatom *Synedra acus* under the effect of colchicine treatment at different stages of the cell cycle. Journal of Structural Biology 190: 73–80. https://doi.org/10.1016/j.jsb.2014.12.004

Kim MS, Park S, Nam O, Lee J, Jin E (2024) Differential expression of silicon transporter genes in frustule formation of the marine diatom *Thalassiosira eccentrica* LIMS-PS-3165. Algae 39(4): 307–318. https://doi.org/10.4490/algae.2024.39.11.22

Kumar S, Rechav K, Kaplan-Ashiri I, Gal A (2020) Imaging and quantifying homeostatic levels of intracellular silicon in diatoms. Science Advances 6(42): eaaz7554. https://doi.org/10.1126/sciadv.aaz7554

Likhoshway YV, Masyukova YA, Sherbakova TA, Petrova DP, Grachev MA (2006) Detection of the gene responsible for silicic acid transport in Chrysophycean algae. Doklady Biological Sciences 408: 256–260. https://doi.org/10.1134/s001249660603015x

Liu Q, Xing Y, Li Y, Wang H, Mi T, Zhen Y, Yu Z (2020) Carbon fixation gene expression in *Skeletonema marinoi* in nitrogen-,phosphate-, silicate-starvation, and low-temperature stress exposure. Journal of Phycology 56: 310–323. https://doi.org/10.1111/jpy.12936

Livak KJ; Schmittgen TD (2001) Analysis of relative gene expression data using real-time quantitative PCR and the 2−ΔΔCT method. Methods 25: 402–408. https://doi.org/10.1006/meth.2001.1262

Malviya S, Scalco E, Audic S, Vincent F, Veluchamy A, Poulain J, Wincker P, Iudicone D, de Vargas C, Bittner L, Zingone A, Bowler C (2016) Insights into global diatom distribution and diversity in the world's ocean. Proceedings of the National Academy of Sciences 113(11): E1516-25. https://doi.org/10.1073/pnas.1509523113

Mann DG, Vanormelingen P (2013) An inordinate fondness? The number, distributions, and origins of diatom species. Journal of Eukaryotic Microbiology 60(4): 414–420. https://doi.org/10.1111/jeu.12047

Marchenkov AM, Bondar AA, Petrova DP, Habudaev KV, Galachyants YP, Zakharova YR, Grachev MA (2016) Unique configuration of genes of silicon transporter in the freshwater pennate diatom *Synedra acus* subsp. *radians*. Doklady Biochemistry and Biophysics 471: 407–409. https://doi.org/10.1134/S1607672916060089

Marchenkov AM, Petrova DP, Morozov AA, Zakharova YR, Grachev MA, Bondar AA (2018) A family of silicon transporter structural genes in a pennate diatom *Synedra ulna*

subsp. *danica* (Kütz.) Skabitsch. PLoS ONE 13(8): e0203161. https://doi.org/10.1371/journal.pone.0203161

Marron AO, Alston MJ, Akam M, Caccamo M, Holland PWH, Walker G (2013) A family of diatom-like silicon transporters in the siliceous loricate choanoflagellates. Proceedings of the Royal Society B: Biological Sciences 280: 1–10. https://doi.org/10.1098/rspb.2012.2543

Marron AO, Ratcliffe S, Wheeler GL, Goldstein RE, King N, Not F, Richter DJ (2016) The evolution of silicon transport in eukaryotes. Molecular Biology and Evolution 33: 3226–3248. https://doi.org/10.1093/molbev/msw209

Martin-Jezequel V, Hildebrand M, Brzezinski MA (2000) Silicon metabolism in diatoms: implications for growth. Journal of Phycology 36: 821–840. http://dx.doi.org/10.1046/j.1529-8817.2000.00019.x

Nielsen FH (2014) Update on the possible nutritional importance of silicon. Journal of Trace Elements in Medicine and Biology 28: 379–382. https://doi.org/10.1016/j.jtemb.2014.06.024

Sapriel G, Quinet M, Heijde M, Jourden L, Tanty V, Luo G, Crom S.L, Lopez PJ (2009) Genom-wide transcriptome analyses of silicon metabolism in *Phaeodactylum tricornutum* reveal the multilevel regulation of silicon acid transporters. PLOS ONE 4(10): e7458. https://doi.org/10.1371/journal.pone.0007458

Shishlyannikov SM, Zakharova YR, Volokitina NA, Mikhailov IS, Petrova DP, Likhoshway YV (2011) A procedure for establishing an axenic culture of the diatom *Synedra acus* subsp. *radians* (Kutz.) Skabibitsch. from Lake Baikal. Limnology and Oceanography: Methods 9: 478–484. https://doi.org/10.4319/lom.2011.9.478

Shrestha RP, Tesson B, Norden-Krichmar T, Federowicz S, Hildebrand M, Allen AE (2012) Whole transcriptome analysis of the silicon response of the diatom *Thalassiosira pseudonana*. BMC Genomics 13: 1–16. https://doi.org/10.1186/1471-2164-13-499

Sullivan CW (1977) Diatom mineralization of silicic acid. II. Regulation of Si(OH)4 transport rates during the cell cycle of *Navicula pelliculosa*. Journal of Phycology 13(1): 86–91. https://doi.org/10.1111/j.1529-8817.1977.tb02892.x

Thamatrakoln K, Alverson AJ, Hildebrand M (2006) Comparative sequence analysis of diatom silicon transporters: toward a mechanistic model of silicon transport. Journal of Phycology 42(4): 822–834. https://doi.org/10.1111/j.1529-8817.2006.00233.x

Thamatrakoln K, Hildebrand M (2007) Analysis of *Thalassiosira pseudonana* silicon transporters indicates distinct regulatory levels and transport activity through the cell cycle. Eukaryotic Cell 6(2): 271–279. https://doi.org/10.1128/EC.00235-06

Thompson AS, Rhodes JC, Pettman I, Wilson T (1988) Culture collection of algae and protozoa: Catalogue of strains. Titus Wilson and Son, Kendal, 164pp.

Tréguer P, Nelson DM, van Bennekom AJ, DeMaster DJ, Leynaert A, Queguiner B (1995) The silica balance in the world ocean: A reestimate. Science 268: 375–379. https://doi.org/10.1126/science.268.5209.375